Supplementary Material

Near-Infrared Optical Spectroscopy In Vivo Distinguishes Subjects with Alzheimer's Disease from Age-Matched Controls

1. Characteristics of tissue scatterers and absorbers in human brain

Supplementary Table 1 summarizes the materials in brain tissue known to scatter and absorb light. We have not established any connection between these materials and the two discriminants discovered for AD-alone and controls.

Supplementary Table 1. Some relevant scatterers and absorbers in human brain [1-6].

Scatterer/ Absorber	Absorption coefficient ($\mu_a(\lambda)$, cm^{-1})	Size (φ, µm)	Refractive index	Relative refractive index
Nuclei		5-7	1.37-1.46	0.996 – 1.07
organelles[§]		$0.1 \leq \varphi \leq 3$	1.38-1.41	1.01 – 1.03
plaque cores		10-13	1.39 – 1.47	1.03-1.11
tangles		$10 \leq \varphi \leq 20$	~1.45	~1.1
Melanin {granules}	~10^2 (800 nm)	{~0.03}	{1.6-1.7}	{1.17 – 1.24}
oxy-hemoglobin[ł]	~10 (800 nm)			
deoxy-hemoglobin[ł]	~10 (800 nm)			
lipid	<10^{-1} (800 nm)			
water	<10^{-2} (800 nm)			

[§]e.g., mitochondria, lysosomes, peroxisomes,
[ł]Reported molar extinction coefficients for oxy- and deoxy-hemoglobin at 800 nm are about 800 – 880 cm^{-1}/M and 762 – 920 cm^{-1}/M respectively [7 and references to tabulated data therein]. Typical hemoglobin concentrations: blood, ~150 g/L; red blood cells ~330 g/L.
λ, wavelength; φ, typical diameter; relative refractive index, n(particle)/n(local environment)

2. Transforming raw data for feature selection

Because the computational programs were written for pixel number rather than wavelength, pixel number will be used here. Calibration with a neon lamp assigned wavelengths to pixel number, here denoted as "p," which is an integer between 1 and 1024.

a. Let f(p) be the raw number of counts collected over the acquisition time, τ.

Let β(p) be the raw number of counts collected for the same τ with the lamp shutter closed, that is, the background counts.

Collect and normalize reference spectrum

b. The reference spectrum is determined by collecting a reflectance spectrum from a "white" surface, either barium sulfate or Spectralon. Then the reference spectrum, r(p), used is

$$r(p) = \frac{f(p) - \beta(p)}{A}$$

where A is the area under f(p) – β(p).

Collect data spectrum and correct for lamp spectrum and acquisition time

c. The raw data collected at the subject's temple are treated as follows to give intensity spectra, I(p):

$$I(p) = \frac{f(p) - \beta(p)}{r(p)\tau}$$

These are the spectra which, after averaging over individuals, are presented in Figure 2 in the main paper. Note the raw data referred to by f(p) and β(p) here are from the subject, whereas the raw data in paragraph b are from the white reference materials.

Compute and smooth area-normalized intensity spectrum

d. Let B be the area under the curve I(p). The area-normalized curve, N(p), is determined as:

$$N(p) = \frac{I(p)}{B}$$

This is done to minimize the effects of the differences of intensity on the first derivatives.

e. N(p) is smoothed by boxcar averaging over 5 pixels, resulting in the new spectrum S(p).

Compute slope variate at each pixel

f. The slope at each pixel of S(p) is calculated as follows:

(1) At each pixel p, fit the line m(p)+b(p) by the method of least squares over the 11 points from p-5 to p+5 where m is the slope and b is the intercept. Clearly, this calculation must begin at pixel 6 and end at pixel 1119.

(2) Form a new spectrum m(p), which will have lost 5 pixels at each end.

g. Feature selection is done on m(p).

3. Details of feature selection technique

Operational definition of fraction-product:

Given spectra on samples from two distinct populations, 1 and 2, at each wavelength (pixel):

1. Determine for sample 1 the median value (M1) of the spectral feature.
2. Determine for sample 2 the median value (M2) of the spectral feature.
3. Assuming that M1 and M2 correspond to the population values, estimate a classification cutoff as (M1 + M2)/2.
4. Determine the fraction of sample 1 on the correct side of the cutoff (f1).
5. Determine the fraction of sample 2 on the correct side of the cutoff (f2).

6. Calculate the fraction-product: fp=f1×f2.

This process assigns a value of fp to each pixel, now 1014 in number because of the algorithm for computing the first derivative (2(f)). The range of fp is from 0.25 (complete overlap of the two distributions) to 1 (complete separation of the two distributions). Feature selection, therefore, looks at those pixels for which the value of fp is near 1. Using the discovery sets for AD-alone (5 subjects) and controls (5 subjects) and proceeding by stepwise decrements from 1:

Cutoff: fp > 0.9 no pixels found

Cutoff: fp > 0.8

pixel	wavelength	fp
483	861.45 nm	0.83
484	861.05 nm	0.83
485	860.64 nm	0.90

Because real optical features (as opposed to random error) have linewidth, we imposed an additional criterion on the candidate features: fp must exceed cutoff on at least 3 contiguous pixels. Therefore, we have discovered one feature, a region around 861 nm. We continue to look for a second feature.

Cutoff: fp > 0.7

pixel	wavelength	fp
398	896.09 nm	0.71
399	895.68 nm	0.71
400	895.28 nm	0.75
483	861.45 nm	0.83

484	861.05 nm	0.83
485	860.64 nm	0.90
486	860.23 nm	0.71
970	665.08 nm	0.73

Now there are two regions of pixels that meet our criteria: 398-400 and 483-486 for fp > 0.7. Although pixel 970 has an fp value above the cut-off, the absence of adjacent pixels with a similarly significant fp value suggests that this is due to random error; this feature was not studied any further.

The two regions of pixels suggest two optical features. In order to reduce the data from 7 pixels to 2, we applied linear discriminant analysis to determine which two pixels used in combination best separate AD-alone from control. Pixels 399 and 485 were determined to give the best separation, and, therefore, became the features used in all subsequent analyses. These two features were extracted from a comparison of AD-alone and control sets. If a similar analysis had been performed on "AD+Lewy bodies" and controls, for example, not only would the features that distinguish AD from control appear but the features that distinguish Lewy bodies from controls would be detected also. These additional features confound those that best separate AD-alone from control.

4. Results from 30 mm source-detector spectra

Both the 25 and 30 mm source-detector separations would be expected to interrogate the temporal lobe. The 30 mm data were analyzed in exactly the same way as the 25 mm data. Feature selection identified the same pixels as best for distinguishing AD-alone from control discovery sets: 399 and 485.

For the 25 mm data, a cut-off may be chosen for Figure 4 such that the sensitivity and specificity are both 100%. The 30 mm data are not as amenable to classification. In the analogous Supplementary Figure 2, any cut-off must make compromises. The cut-off illustrated in Supplementary Figure 2 results in a sensitivity of 95% (AD considered positive) and a specificity of 85%.

In Student's t-test, the number of degrees of freedom is usually considered to be N-1, where N is the number of observations. The Hotelling T2 test generalizes Student's t-test to the case in which more than one quantity is measured [8]. For the two-sample Hotelling T2 test, the number of degrees of freedom is N1 + N2 - p – 1, where p is the number of quantities measured; N1 and N2 are the numbers of subjects in each sample. In Supplementary Figure 2, p =2; N1=8 (controls); N2=15 (AD). So, the number of degrees of freedom is 20, and the significance of T2 takes into consideration the small numbers of subjects involved. Substituting p=1 in the formula for the T2 test above reduces it to the usual formula for Student's t: (N1-1) + (N2-1).

REFERENCES

[1] Kalashnikov M, Choi W, Yu CC, Sung Y, Dasari RR, Badizadegan K, Feld MS (2009) Assessing light scattering of intracellular organelles in single intact living cells. *Opt Express* **17**, 19674-19681.

[2] Hyman BT, West HL, Rebeck GW, Buldyrev SV, Mantegna RN, Ukleja M, Havlin S, Stanley HE (1995) Quantitative analysis of senile plaques in Alzheimer disease: observation of log-normal size distribution and molecular epidemiology of differences associated with apolipoprotein E genotype and trisomy 21 (Down syndrome). *Proc Natl Acad Sci U S A* **92**, 3586-3590.

[3] Tuchin VV (2015) Tissue optics and photonics: light-tissue interaction. *J Biomed Photonics Eng* **1**, 98-134.

[4] Zecca L, Bellei C, Costi P, Albertini A, Monzani E, Casella L, Gallorini M, Bergamaschi L, Moscatelli A, Turro NJ, Eisner M, Crippa PR, Ito S, Wakamatsu K, Bush WD, Ward WC, Simon JD, Zucca FA (2008) New melanic pigments in the human brain that accumulate in aging and block environmental toxic metals. *Proc Natl Acad Sci U S A* **105**, 17567-17572.

[5] DeTure MA, Dickson DW (2019) The neuropathological diagnosis of Alzheimer's disease. *Mol Neurodegener* **14**, 32.

[6] Nelson PT, Alafuzoff I, Bigio EH, Bouras C, Braak H, Cairns NJ, Castellani RJ, Crain BJ, Davies P, Del Tredici K, Duyckaerts C, Frosch MP, Haroutunian V, Hof PR, Hulette CM, Hyman BT, Iwatsubo T, Jellinger KA, Jicha GA, Kövari E, Kukull WA, Leverenz JB, Love S, Mackenzie IR, Mann DM, Masliah E, McKee AC, Montine TJ, Morris JC, Schneider JA, Sonnen JA, Thal DR, Trojanowski JQ, Troncoso JC, Wisniewski T, Woltjer RL, Beach TG (2012) Correlation of Alzheimer disease neuropathologic changes with cognitive status: a review of the literature. *J Neuropathol Exp Neurol* **71**, 362-381.

[7] Zhao Y, Qiu L, Sun Y, Huang C, Li T (2017) Optimal hemoglobin extinction coefficient data set for near-infrared spectroscopy. *Biomed Optics Express* **8**, 5151–5159.

[8] Hotelling H (1931) The generalization of Student's ratio. *Ann Math Stat* **2**, 360-378.

Supplementary Figure 1. 30 mm source-detector separation scatter plot of selected AD and control subjects. Feature selection on the 30 mm spectra resulted in choosing the same two slope variates as the 25 mm data. This figure corresponds exactly to Figure 3 and indicates similar results, although the separation of the two groups is not as clear. Parenthetical number is the number of subjects in that group.

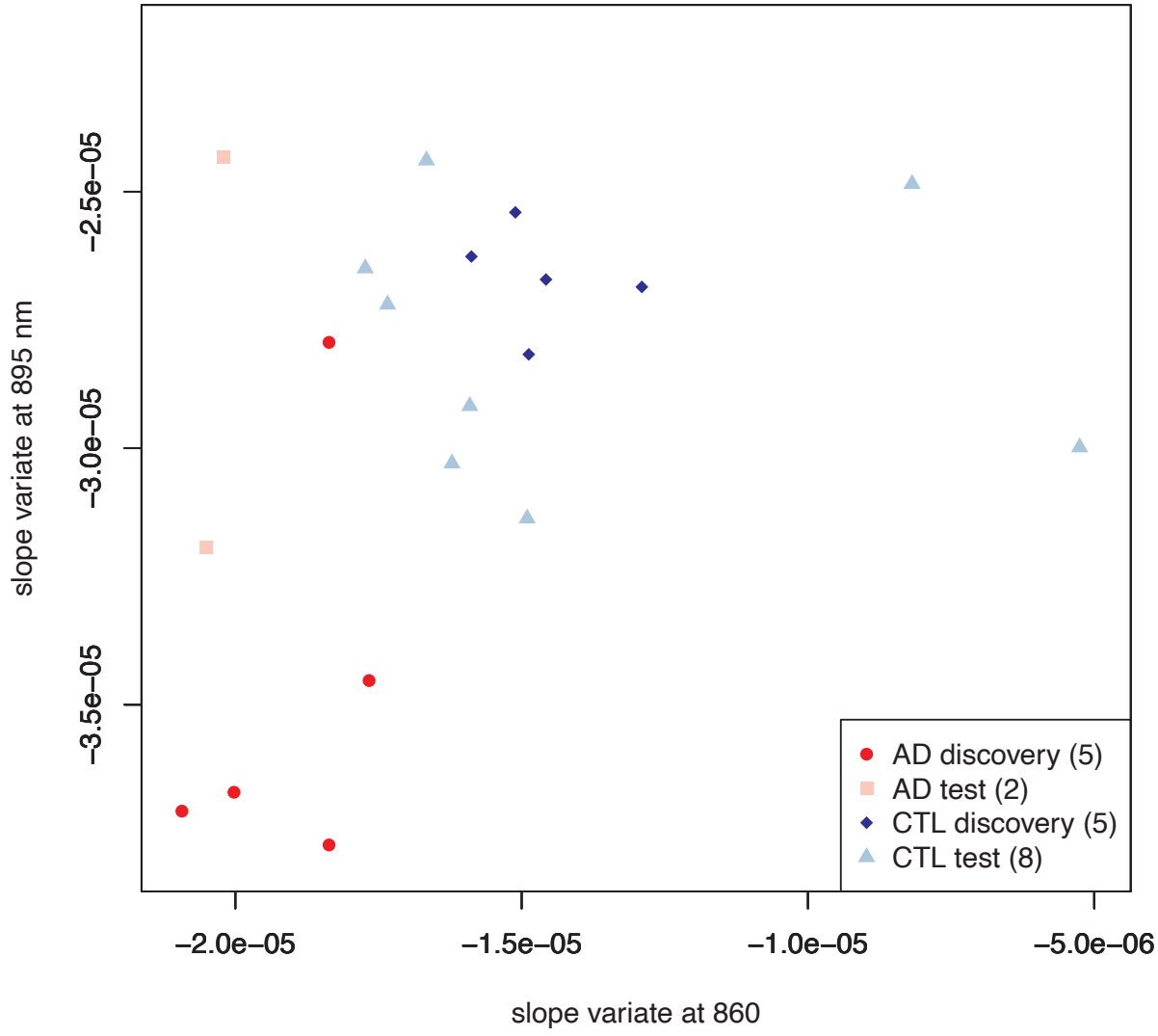

Supplementary Figure 2. 30 mm source-detector separation scatter plot adding AD subjects with additional pathology. This diagram is analogous to Figure 4 and shows similar results, although there is some overlap of the two groups. The separation of the two groups of "test" subjects remains statistically significant ($p < 0.003$; Hotelling T2 test). Parenthetical number is the number of subjects in that group.

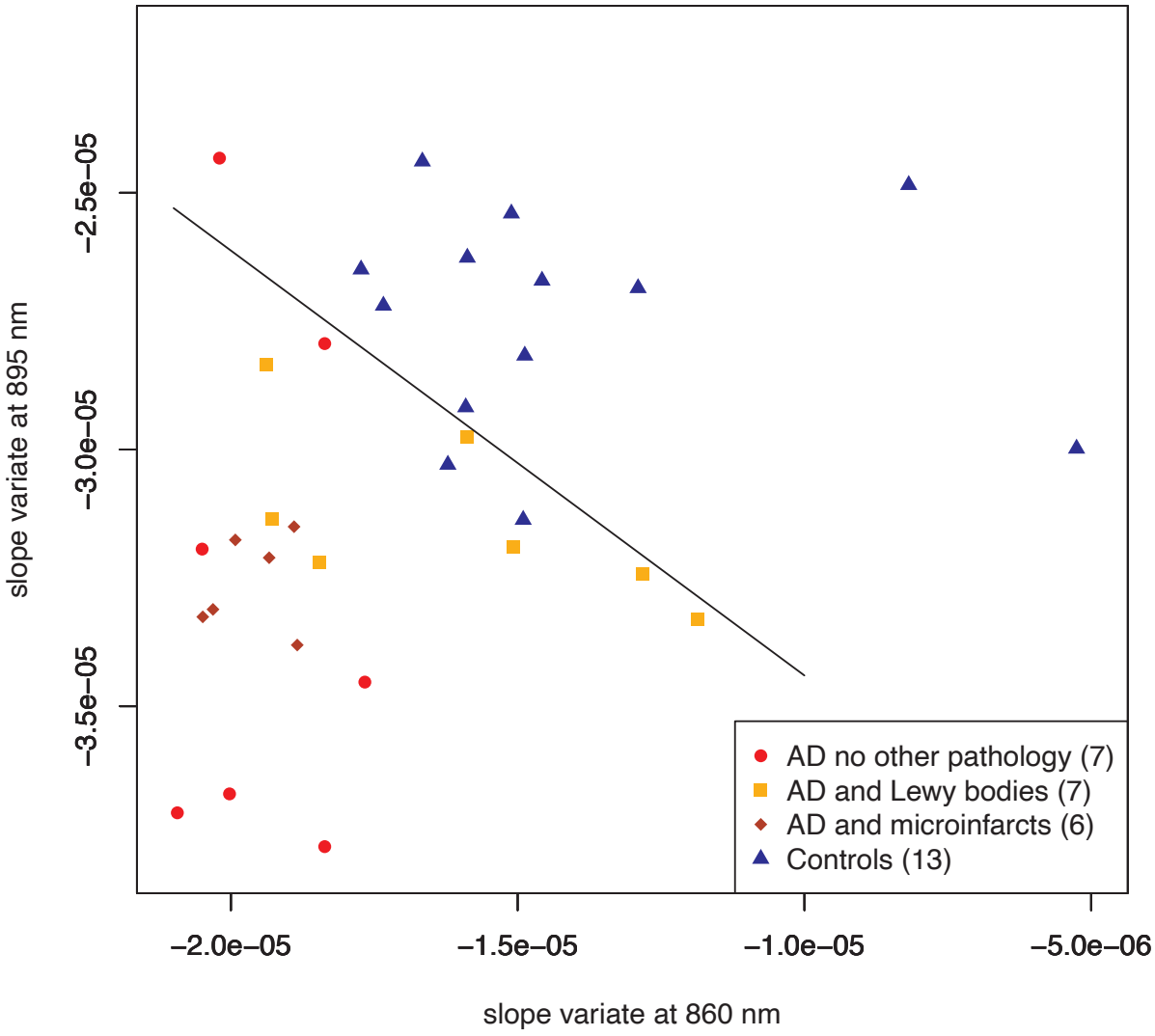

Supplementary Figure 3. 30 mm source-detector separation principal component analysis of MCI, control and AD without other pathology subjects. These plots correspond to those of Figure 6. Most importantly, the scores separate the MCI subjects into two clusters (right panel) that answer to the clinical assessment of the degree of cognitive impairment. Using the scores as a measure, the difference between the two groups is statistically significant ($p < 0.03$; Welch t-test). Parenthetical number is the number of subjects in that group.